Systematic calculations of cluster radioactivity half-lives in trans-lead nuclei*

Lin-Jing Qi(亓林静)[1] Dong-Meng Zhang(张冬萌)[1] Song Luo(骆松)[1] Xiao-Hua Li(李小华)[1,4,5†]
Xi-Jun Wu(吴喜军)[2‡] Chun-Tian Liang(梁春恬)[3§]

[1]School of Nuclear Science and Technology, University of South China, Hengyang 421001, China
[2]School of Math and Physics, University of South China, Hengyang 421001, China
[3]School of Science, Tianjin Chengjian University, Tianjin 300384, China
[4]Cooperative Innovation Center for Nuclear Fuel Cycle Technology & Equipment, University of South China, Hengyang 421001, China
[5]Key Laboratory of Low Dimensional Quantum Structures and Quantum Control, Hunan Normal University, Changsha 410081, China

Abstract: In the present work, based on the Wentzel-Kramers-Brillouin (WKB) theory, considering the cluster preformation probability (P_c), we systematically investigate the cluster radioactivity half-lives of 22 trans-lead nuclei ranging from ^{221}Fr to ^{242}Cm. When the mass number of the emitted cluster $A_c < 28$, P_c is obtained by the exponential relationship of P_c to the α decay preformation probability (P_α) proposed by R. Blendowskeis *et al.* [Phys. Rev. Lett. **61**, 1930 (1988)], while P_α is calculated through the cluster-formation model (CFM). When $A_c \geq 28$, P_c is calculated through the charge-number dependence of P_c on the decay products proposed by Ren *et al.* [Phys. Rev. C **70**, 034304 (2004)]. The half-lives of cluster radioactivity have been calculated by the density-dependent cluster model [Phys. Rev. C **70**, 034304 (2004)] and by the unified formula of half-lives for alpha decay and cluster radioactivity [Phys. Rev. C **78**, 044310 (2008)]. For comparison, a universal decay law (UDL) proposed by Qi *et al.* [Phys. Rev. C **80**, 044326 (2009)], a semi-empirical model for both α decay and cluster radioactivity proposed by Santhosh [J. Phys. G: Nucl. Part. Phys. **35**, 085102 (2008)], and a unified formula of half-lives for alpha decay and cluster radioactivity [Phys. Rev. C **78**, 044310 (2008)] are also used. The calculated results of our work, Ni's formula , and the UDL can well reproduce the experimental data and are better than those of Santhosh's model. In addition, we extend this model to predict the half-lives for 51 nuclei, whose cluster radioactivity is energetically allowed or observed but not yet quantified in NUBASE2020.

Keywords: cluster radioactivity, cluster-formation model (CFM), half-lives, preformation probability

DOI: 10.1088/1674-1137/ac94bd

I. INTRODUCTION

In nature, radioactive nuclei translate their unstable states to stable states, based on the minimum energy principle, by α, β, and/or γ emissions, or emitting particles heavier than α particles [1–3] but lighter than the lightest fission fragments, generally known as cluster radioactivity [4–10]. This subtle process, intermediate between α decay and spontaneous fission, undoubtedly involves vital nuclear structure information such as ground state half-life time, nuclear spin and parity, deformations of nuclear structure, and shell effects [11–13]. In 1980, Săndulescu, Poenaru, and Greiner first predicted this type of decay mode [14–17]. Experiments conducted by Rose and Jones in 1984 [15, 17], for observing ^{14}C emitted particles from ^{223}Ra, verified the realistic existence of this novel radioactivity. Soon afterwards, multiple extra elementary clusters such as ^{20}O, ^{24}Ne, ^{23}F, ^{28}Mg and ^{34}Si were discovered experimentally in the trans-lead region [18, 19], leading to the doubly magic daughter nucleus ^{208}Pb or its neighboring nuclei.

Up to now, abundant theoretical models have been proposed to deal with this radioactivity process. In general, these models can be divided into two kinds of categories, α-like models and fission-like models [20–23], by virtue of the intermediate characteristics. The former, just

Received 12 July 2022; Accepted 26 September 2022; Published online 11 October 2022

* This work is supported in part by the National Natura Science Foundation of China (12175100 and 11975132), the Construct Program of the Key Discipline in Hunan Province, the Research Foundation of Education Bureau of Hunan Province (18A237), the Natural Science Foundation of Hunan Province (2018JJ3324), the Innovation Group of Nuclear and Particle Physics in USC, the Shandong Province Natural Science Foundation (ZR2015AQ007), the National Innovation Training Foundation of China (201910555161), and the Opening Project of Cooperative Innovation Center for Nuclear Fuel Cycle Technology and Equipment, University of South China (2019KFZ10).

† E-mail: lixiaohuaphysics@126.com
‡ E-mail: wuxijun1980@yahoo.cn
§ E-mail: chuntianliang@hotmail.com

like the tunnelling theory of α decay [24–27], considering this process as non-adiabatic process, supposes the cluster is preformed in the parent nucleus with a certain cluster formation probability, determined by the overlapping region of both the parent nucleus and the daughter nucleus before they could penetrate the barrier with an available decay energy of cluster radioactivity Q_c [28]. For instance, in 2001, considering nuclear proximity energy and quasimolecular shape, Royer generalized the conventional liquid drop model (GLDM) [23] to systematically calculate the cluster radioactivity half-lives. Soon afterwards, considering the cluster preformation factor P_c as the charge-number dependence form, Ren *et al.* employed the microscopic density-dependent cluster model (DDCM) where the realistic M3Y nucleon-nucleon interaction is used to investigate this exotic decay mode [14]. In 2009, extending the quasi-bound wave function, first used in α decay, to cluster radioactivity, based on the DDCM, Ni *et al.* systematically studied the half-lives of cluster radioactivity [4]. In the latter, the cluster is assumed to be formed along with the emitted process, which is described as adiabatic with constant variations in geometric shape from the parent nucleus during its penetration through the nuclear barrier. Based on this assumption, in 2013, Santhosh *et al.* used the Coulomb and proximity potential model (CPPM) to calculate the half-lives of α decay and cluster radioactivity of $^{248-254}$Cf isotopes for the purpose of exploring the stability of these nuclei against these decay modes [21]. Recently, Ajeet Singh *et al.* used the effective liquid drop model (ELDM) as well as the mass excess data calculated by the relativistic mean-field (RMF) to study cluster radioactivity half-lives [29]. In addition, many phenomenological semi-empirical formulas have been proposed to deal with this phenomenon. For instance, Ni *et al.* proposed a unified formula of half-lives for both α decay and cluster radioactivity in 2008 [30]. All of them can explicitly elaborate this exotic decay mode and provide a reliable theoretical foundation for future research.

No matter in which theory, P_c plays an indispensable role in calculating cluster radioactivity half-lives. Different models have different methods to deal with P_c. In the preformed cluster model (PCM) [31, 32] proposed by Gupta and Malik, P_c is calculated through solving the stationary Schrödinger equation for the dynamical flow of mass and charge. In terms of fission-like models, P_c is regarded as the penetrability of the inner part of the barrier for the overlapping region. As for the unified fission model (UFM) [33], P_c is usually considered as unity. Based on the fact that the α particle is an $N=Z$ system with a larger binding energy, it is reasonable to deem the preformation probability just as 1 within Gamow's theory for α decay. Nevertheless, as in the case of cluster radioactivity, the emitted particles in the whole cluster family are completely $N\neq Z$ systems. The more nucleons aggregate as a cluster, the less the possibility exists in the parent nucleus [34]. Therefore, when the UFM is applied to calculate cluster radioactivity half-lives, the preformation probability, assumed to be 1, may be reevaluated. To this end, based on the Wentzel-Kramers-Brillouin (WKB) theory, considering cluster radioactivity preformation probability P_c, we systematically investigate the cluster radioactivity half-lives of 22 trans-lead nuclei ranging from ^{221}Fr to ^{242}Cm, while the interaction potential between the emitted cluster and daughter nucleus in the overlapping region is a sum of the repulsive Coulomb potential $V_C(r)$, a modified Woods-Saxon type nuclear potential $V_N(r)$, and the centrifugal potential $V_l(r)$. As for P_c, when $A_c<28$ we calculate it within the cluster-formation model (CFM) [35–37] combined with the famous exponential relationship of P_c to P_α proposed by R. Blendowske and H. Walliser [38]. However, with A_c going beyond the limit this relationship may not work [39]. As is clearly indicated in Fig. 2 from Ref. [39], P_c in logarithmical form maintains a good linear relationship with the mass number of the emitted cluster when $A_c<28$. The curve is bent obviously when $28<A_c\leq40$ and the slope of the curve begins to decrease with increasing emitted cluster mass number. Therefore, in this work, when $A_c\geq28$, P_c is obtained by its charge-number dependence on the decay products in the DDCM proposed by Ren *et al.* [14].

This article is organized as follows. A brief introduction to the theoretical framework for cluster radioactivity half-life, CFM, and semi-empirical formulas is presented in Sec. II. Detailed numerical results and discussion are given in Sec. III. Sec. IV is a simple summary.

II. THEORETICAL FRAMEWORK

A. Half-lives of the cluster radioactivity

The half-life for the cluster radioactivity is defined as [40]

$$T_{1/2}=\frac{\ln 2}{\lambda}, \tag{1}$$

where λ is denoted as the decay constant determined as the product of the penetration probability P, the assault frequency ν, and the cluster-preformation probability P_c. It can be expressed as [41]

$$\lambda=\nu P P_c. \tag{2}$$

Here, P is the penetrability of the cluster crossing the barrier, which is calculated by the Wentzel-Kramers-Brillouin (WKB) approximation. It can be expressed as

$$P = \exp\{-\frac{2}{\hbar}\int_{R_{in}}^{R_{out}}\sqrt{2\mu(V(r)-Q_c)}\mathrm{d}r\}, \tag{3}$$

where $\hbar$ is the reduced Planck constant. $\mu = \frac{M_c M_d}{M_c + M_d}$ is the reduced mass of the emitted cluster-daughter nucleus system with M_c and M_d being the masses of the emitted cluster and daughter nuclei, respectively [42]. R_{in}=C_1+C_2 [34] is the saddle point for the touching configuration with C_i=$R_i\left(1-\frac{b^2}{R_i^2}\right)$ (i=1,2) being the S ü ssmann central radii [43] of the daughter and cluster nucleus on account of the surface correction to the sharp radius R_i. b=1 fm is the diffuseness parameter of the nuclear surface taken from Ref. [44]. The sharp radius R_i, is given by [45]

$$R_i = 1.28A_i^{1/3} - 0.76 + 0.8A_i^{-1/3}, \tag{4}$$

where A_i $(i = c,d)$ are the mass number of the emitted cluster and daughter nucleus, respectively. R_{out} is the outer turning point of the barrier and satisfies the condition $V(R_{out}) = Q_c$ [5]. In this work, Q_c can be obtained by

$$Q_c = B(A_c,Z_c) + B(A_d,Z_d) - B(A,Z), \tag{5}$$

where $B(A_c,Z_c)$, $B(A_d,Z_d)$ and $B(A,Z)$ are, respectively, the binding energies of the emitted cluster, daughter, and parent nuclei taken from AME2020 [46] and NUBASE2020 [47] with Z_c, Z_d and Z being the proton numbers of the emitted cluster, daughter, and parent nuclei and A being the mass number of the parent nucleus.

The $V(r)$ in Eq. (3) is the total interacting potential between the emitted cluster and the daughter nucleus including nuclear, Coulomb, and centrifugal potential barriers. It can be written as

$$V(r) = V_N(r) + V_C(r) + V_l(r), \tag{6}$$

where $V_N(r)$ is the nuclear potential. In this work, we choose it as a Woods-Saxon form [22], which can be expressed as

$$V_N(r) = \frac{V_0}{1+\exp\left[\frac{r-R_0}{a}\right]} \tag{7}$$

with

$$R_0 = r_c + r_d - 1.37. \tag{8}$$

Here, $r_i (i = c,d)$ are the nuclear charge radii. They can be expressed as

$$r_i = 1.27A_i^{1/3},\ i = c,d. \tag{9}$$

The potential depth V_0 and diffuseness a are parameterized as [22]

$$V_0 = -44.16[1-0.4(I_d+I_c)]\frac{A_d^{1/3}A_c^{1/3}}{A_d^{1/3}+A_c^{1/3}}, \tag{10}$$

$$a = 0.5 + 0.33I_d. \tag{11}$$

Here, I_i=$\frac{N_i - Z_i}{A_i}$ $(i = c,d)$ are the relative neutron excess of the emitted cluster and daughter nucleus with N_i and Z_i $(i = c,d)$ being the neutron numbers of the emitted cluster and daughter nuclei, respectively. V_C is the Coulomb potential of a uniformly charged sphere, which can be given by

$$V_C(r) = \frac{e^2 Z_c Z_d}{r}, \tag{12}$$

where $e^2 = 1.4399652\ \mathrm{MeV\cdot fm}$ is the square of the electronic elementary charge [17].

V_l in Eq. (3) is the centrifugal potential. In this work, we choose it as the Langer modified form since $l(l+1) \to (l+\frac{1}{2})^2$ is a necessary correction for one-dimensional problems [41]. It can be written as

$$V_l(r) = \frac{\hbar^2\left(l+\frac{1}{2}\right)^2}{2\mu r^2}, \tag{13}$$

where l is the angular momentum carried by the emitted cluster. It can be obtained by

$$l = \begin{cases} \Delta_j, & \text{for even } \Delta_j \text{ and } \pi_p = \pi_d, \\ \Delta_j + 1, & \text{for even } \Delta_j \text{ and } \pi_p \neq \pi_d, \\ \Delta_j, & \text{for odd } \Delta_j \text{ and } \pi_p \neq \pi_d, \\ \Delta_j + 1, & \text{for odd } \Delta_j \text{ and } \pi_p = \pi_d, \end{cases} \tag{14}$$

where $\Delta_j = |j_p - j_d - j_c|$, $j_c,\pi_c,j_p,\pi_p,j_d,\pi_d$ represent the isospin and parity values of the emitted cluster, parent, and daughter nuclei, respectively.

The cluster moves back and forth inside the parent nucleus with a certain speed before penetrating the barrier. For the purpose of evaluating assaults per unit time for the ground state, ν is presented as [48, 49]

$$\nu = \frac{\pi\hbar}{2\mu R_{in}^2}. \tag{15}$$

For the preformation probability P_c, when the mass number of the cluster $A_c < 28$, it can be expressed as [38]

$$P_c = [P_\alpha]^{\frac{(A_c-1)}{3}}, \tag{16}$$

where P_α is the α decay preformation probability. In this work, it is obtained by the CFM [50]. For completeness, detailed information on the CFM is presented in the next subsection. When the mass number of the cluster $A_c \geq 28$, the exponential relationship of P_c to P_α may not work [39]. Therefore, in this work, P_c is calculated through an empirical formula proposed by Ren *et al.* [14] for $A_c \geq 28$. It can be expressed as

$$\log_{10}P_c = \begin{cases} -(0.01674Z_cZ_d - 2.035466), \\ \text{for even}-\text{even nuclei} \\ -(0.01674Z_cZ_d - 2.035466) - 1.175, \\ \text{for odd}-A\text{ nuclei.} \end{cases} \tag{17}$$

B. Cluster-formation model

In CFM, the total initial clusterization state ψ of the considered emitted cluster-daughter nucleus system is a linear combination of all its n possible clusterization ψ_i states [50]

$$\psi = \sum_i^N a_i\psi_i, \tag{18}$$

$$a_i = \int \psi_i^*\psi \mathrm{d}\tau, \tag{19}$$

where a_i is the superposition coefficient of ψ_i, on account of the orthogonality condition [51]

$$\sum_i^N |a_i|^2 = 1. \tag{20}$$

The total Hamiltonian H consists of the accordingly different clusterization configuration [52]. It can be expressed as

$$H = \sum_i^N H_i, \tag{21}$$

where H_i is the i-th Hamiltonian of clusterization state ψ_i. On account of all the clusterizations describing the same nucleus, they are assumed to share the same total energy E of the total wave function [51]. Furthermore, considering the orthonormality of the clusterization wave functions, E can be written as

$$E = \sum_i^N |a_i|^2 E = \sum_i^N E_{f_i}, \tag{22}$$

where E_{f_i} is the formation energy for the cluster in clusterization state ψ_i. Therefore, the α decay preformation probability P_α can be obtained by [50, 52, 53]:

$$P_\alpha = |a_\alpha|^2 = \frac{E_{f_\alpha}}{E}. \tag{23}$$

Here, a_α and E_{f_α} are, respectively, the coefficient of the α clusterization state and the formation energy of the α particle. The α formation energy E_{f_α} and total system energy E can be classified as four different cases in the following expressions [35, 51]:

Case I for even-even nuclei:

$$\begin{aligned} E_{f_\alpha} =& 3B(A,Z) + B(A-4,Z-2) \\ & - 2B(A-1,Z-1) - 2B(A-1,Z), \end{aligned} \tag{24}$$

$$E = B(A,Z) - B(A-4,Z-2). \tag{25}$$

Case II for even-odd nuclei:

$$\begin{aligned} E_{f_\alpha} =& 3B(A-1,Z) + B(A-5,Z-2) \\ & - 2B(A-2,Z-1) - 2B(A-2,Z), \end{aligned} \tag{26}$$

$$E = B(A,Z) - B(A-5,Z-2). \tag{27}$$

Case III for odd-even nuclei:

$$\begin{aligned} E_{f_\alpha} =& 3B(A-1,Z-1) + B(A-5,Z-3) \\ & - 2B(A-2,Z-2) - 2B(A-2,Z-1), \end{aligned} \tag{28}$$

$$E = B(A,Z) - B(A-5,Z-3). \tag{29}$$

Case IV for odd-odd nuclei:

$$\begin{aligned} E_{f_\alpha} =& 3B(A-2,Z-1) + B(A-6,Z-3) \\ & - 2B(A-3,Z-2) - 2B(A-3,Z-1), \end{aligned} \tag{30}$$

$$E = B(A,Z) - B(A-6,Z-3). \tag{31}$$

C. Semi-empirical formula

1. *Universal decay law*

In 2009, using the microscopic mechanism of the

charged-particle emission within α-like R-matrix theory, Qi *et al.* [54, 55] proposed the universal decay law (UDL). It can be expressed as

$$\log_{10}(T_{1/2})(s) = aZ_cZ_d\sqrt{\frac{\mathcal{A}}{Q_c}} + b\sqrt{\mathcal{A}Z_cZ_d(A_c^{1/3}+A_d^{1/3})} + c, \tag{32}$$

where $\mathcal{A}=\frac{A_cA_d}{A_c+A_d}$ is the reduced mass of the emitted cluster-daughter nucleus system measured in units of the nucleon mass. $a = 0.4314$, $b = -0.3921$, and $c = -32.7044$ are the adjustable parameters.

2. *Santhosh's semi-empirical model for α decay and cluster radioactivity*

Based on the Geiger-Nuttall (G-N) law, considering the mass asymmetry, Santhosh *et al.* proposed a formula for estimating the half-lives of α decay and cluster radioactivity in 2008 [56]. It can be given by

$$\log_{10}(T_{1/2})(s) = aZ_dZ_cQ_c^{-1/2} + b\eta_A + c, \tag{33}$$

where $\eta_A=\frac{A_d-A_c}{A}$ is the mass asymmetry. The values of the three adjustable parameters are $a = 0.727356$, $b = 40.3887$ and $c = -85.1625$, respectively.

3. *Unified formula of half-lives for α decay and cluster radioactivity*

Deduced from the WKB barrier penetration probability with some approximation, Ni *et al.* have proposed a unified formula of half-lives for both α decay and cluster radioactivity [30]. It can be expressed as

$$\log_{10}(T_{1/2})(s) = a\sqrt{\mathcal{A}}Z_dZ_cQ_c^{-1/2} + b\sqrt{\mathcal{A}}(Z_dZ_c)^{1/2} + c, \tag{34}$$

where $a = 0.38617$, $b = -1.08676$, $c_{e-e} = -21.37195$, and $c_{\mathrm{odd}-A} = -20.11223$ are the adjustable parameters, respectively.

III. RESULTS AND DISCUSSION

Based on the Wentzel-Kramers-Brillouin (WKB) theory, considering the cluster preformation probability P_c, we systematically calculate the cluster radioactivity half-lives of 22 nuclei in the emission of clusters ^{14}C, ^{15}N, ^{20}O, ^{23}F, ^{24,25,26}Ne, ^{28,30}Mg, and ^{32,34}Si from various parent nuclei ^{221}Fr, $^{221-226}$Ra, ^{223,228,230}Th, ^{231}Pa, $^{232-234}$U, ^{236,238}Pu, and ^{242}Cm resulting in doubly magic ^{208}Pb and its neighboring nuclei in this work. The experimental cluster radioactivity half-lives $T_{1/2}^{\mathrm{exp}}$ are extracted from Ref. [4] and Ref. [22]. The detailed calculated results are given in Table 1. This table is divided into Part I and Part II, which are characterized by $A_c < 28$ and $A_c \geq 28$, respectively. In Table 1, the first to fourth columns represent the decay process, the cluster radioactivity decay energy Q_c, angular momentum l carried by the emitted cluster, and the experimental cluster radioactivity half-lives in logarithmical form, respectively denoted as Decay, Q_c, l and Exp. The fifth to seventh columns are the calculated results of UDL, Santhosh's semi-empirical model, and Ni's formula in logarithmical form, denoted as UDL, Santhosh and Ni, respectively. In our work, P_c is calculated through the exponential relationship of P_c to P_α for $A_c < 28$ with P_α obtained by CFM. Nevertheless, since the exponential relationship of P_c to P_α may break down when $A_c \geq 28$, P_c is calculated through the charge-number dependence of P_c on the decay products in DDCM proposed by Ren *et al.* [14]. The calculated half-life results in logarithmical form are given in the eighth column denoted as Cal^1. For comparison, the theoretical half-life calculations based on WKB theory with P_c being calculated through the same charge-number dependence of P_c when $A_c < 28$ are also presented in the ninth column denoted as Cal^2. From this table, it is clear that the calculated half-life results using Ni's formula, Cal^1, Cal^2 , and UDL are basically in agreement with the experimental data. The results in Cal^1 are better than those in Cal^2 when $A_c < 28$.

For the sake of intuitively comparing these results, we plot the differences between the experimental cluster radioactivity half-lives and the calculated ones by using the UDL, Santhosh's model, Ni's formula, Cal^1, and Cal^2 in logarithmical form in Fig. 1. From this figure, it is clear that the differences between the experimental data and the calculated results in Cal^1 and Ni's formula are within ±2 on the whole, showing that the calculated cluster radioactivity half-lives in Cal^1 as well as Ni's formula can reproduce the experimental data well. By contrast, in the case of ^{223}Ra$\rightarrow$^{209}Pb+^{14}C, there is a discrepancy of 2.482 the UDL. For ^{223}Ac$\rightarrow$^{209}Bi+^{14}C, there is a discrepancy of 2.325 in Cal^2. The values of the discrepancies of 7 of the 22 nuclei are out of the scale of ± 2 within Santhosh's model. Notably, for ^{231}Pa$\rightarrow$^{208}Pb+^{23}F and ^{242}Cm $\rightarrow$^{208}Pb+^{34}Si, the discrepancies reach 4.31 and 5.71, respectively. Furthermore, from the overall trend, the results in Cal^1 converge more on the neighboring zero line area, relatively similar to the distribution of the UDL and Ni's formula. Nevertheless, the distribution of the results of Santhosh's model is slightly scattered. For further investigating the consistencies between the cluster radioactivity half-lives experimental data and the calculated ones obtained by UDL, Santhosh's model, Ni's formula, Cal^1, and Cal^2, the standard deviation σ is used, which is defined by

Table 1. Comparisons between the experimental cluster radioactivity half-lives (in seconds) and the calculated ones using the UDL, Santhosh's model, Ni's formula, and our model in logarithmic form.

Decay	Q_c/MeV	l	$\log_{10}T_{1/2}$ (s)					
			Exp	UDL	Santhosh	Ni	Cal[1]	Cal[2]
Part I: $A_c < 28$								
^{221}Fr$\rightarrow$ ^{207}Tl+^{14}C	31.2911	3	14.56	12.70	13.30	14.63	14.76	16.37
^{221}Ra$\rightarrow$ ^{207}Pb+^{14}C	32.3961	3	13.39	11.46	12.98	13.48	13.55	15.31
^{222}Ra$\rightarrow$ ^{208}Pb+^{14}C	33.0486	0	11.22	10.07	12.38	11.02	12.10	12.77
^{223}Ra$\rightarrow$ ^{209}Pb+^{14}C	31.8279	4	15.05	12.57	13.59	14.56	14.75	16.20
^{224}Ra$\rightarrow$ ^{210}Pb+^{14}C	30.5343	0	15.87	15.38	14.94	15.86	16.91	17.43
^{226}Ra$\rightarrow$ ^{212}Pb+^{14}C	28.1966	0	21.20	20.95	17.62	20.94	21.89	22.39
^{223}Ac$\rightarrow$ ^{209}Bi+^{14}C	33.0636	2	12.60	11.07	13.15	13.19	13.31	14.93
^{228}Th$\rightarrow$ ^{208}Pb+^{20}O	44.7233	0	20.73	21.97	19.49	21.54	21.44	22.39
^{231}Pa$\rightarrow$ ^{208}Pb+^{23}F	51.8828	1	26.02	24.90	21.71	25.59	24.06	22.39
^{230}Th$\rightarrow$ ^{206}Hg+^{24}Ne	57.7599	0	24.63	25.39	23.36	24.58	23.57	25.82
^{231}Pa$\rightarrow$ ^{207}Tl+^{24}Ne	60.4099	1	22.89	22.27	22.64	23.09	21.54	25.21
^{232}U$\rightarrow$ ^{208}Pb+^{24}Ne	62.3095	0	20.39	20.59	22.43	20.36	19.73	23.86
^{233}U$\rightarrow$ ^{209}Pb+^{24}Ne	60.4853	2	24.84	23.63	23.60	24.41	23.02	21.35
^{234}U$\rightarrow$ ^{210}Pb+^{24}Ne	58.8250	0	25.93	26.52	24.71	25.81	25.01	25.06
^{233}U$\rightarrow$ ^{208}Pb+^{25}Ne	60.7036	2	24.84	24.00	23.11	24.88	23.40	25.15
^{234}U$\rightarrow$ ^{208}Pb+^{26}Ne	59.4125	0	25.93	27.01	23.63	26.52	25.53	26.21
Part I: $A_c \geq 28$								
^{234}U$\rightarrow$ ^{206}Hg+^{28}Mg	74.1108	0	25.53	25.77	26.67	25.25	25.76	–
^{236}Pu$\rightarrow$ ^{208}Pb+^{28}Mg	79.6700	0	21.52	20.64	25.83	20.76	21.81	–
^{238}Pu$\rightarrow$ ^{210}Pb+^{28}Mg	75.9114	0	25.70	26.26	27.87	25.96	26.28	–
^{238}Pu$\rightarrow$ ^{208}Pb+^{30}Mg	76.7930	0	25.70	26.06	26.72	26.10	25.75	–
^{238}Pu$\rightarrow$ ^{206}Hg+^{32}Si	96.1867	0	25.28	25.48	29.68	25.59	26.00	–
^{242}Cm $\rightarrow$ ^{208}Pb+^{34}Si	96.5440	0	23.15	22.35	28.86	23.48	23.43	–

$$\sigma = \left[\sum_{i}^{n}(\log_{10}T_{1/2_i}^{\rm exp} - \log_{10}T_{1/2_i}^{\rm cal})^2/n\right]^{1/2}, \qquad (35)$$

where $\log_{10}T_{1/2_i}^{\rm exp}$ and $\log_{10}T_{1/2_i}^{\rm cal}$ denote the logarithmic form of the experimental cluster radioactivity half-lives and calculated ones for the i-th nucleus, respectively. The calculated results of σ using the UDL, Santhosh's model, Ni's formula, Cal[1], and Cal[2] are presented in Table 2. From this table, as $A_c < 28$, the σ value between the experimental data and the results obtained in CFM is 1.035, smaller compared to the results from Cal[2], UDL, and Santhosh's model, which are 1.256, 1.244, and 1.880, respectively, larger than the results from Ni with 0.365. As $A_c \geq 28$, the σ values of Cal[1] and Ni's formula are 0.423 and 0.425, smaller than those from the UDL and Santhosh's model, which are 0.569 and 3.594, respectively. For the total nuclei, it is clear that σ between the experimental data and the results calculated in Cal[1] is 0.910, a better result than those resulting from the UDL and Santhosh's model, which are 1.102 and 2.469, respectively, closer to Ni's formula with 0.382, which is the least. Moreover, the calculated results in Cal[1] are better than the ones based on different types of proximity potentials from Ref. [57], where the standard deviation σ between experimental and calculated half-lives ranges from 1.373 up to 7.951. This indicates that the our calculated cluster radioactivity half-lives results can reproduce the experimental data well. However, as for ^{231}Pa $\rightarrow$ ^{208}Pb+^{23}F with a discrepancy of 1.962 and ^{233}U $\rightarrow$ ^{209}Pb+^{24}Ne with a discrepancy of 1.825, the experimental data can not be properly reproduced. This may account for the imperfection of early detection technologies and radioactive beam equipment.

Encouraged by the good agreement between the experimental cluster radioactivity half-lives and the calculated ones within our model, in the following, we extend

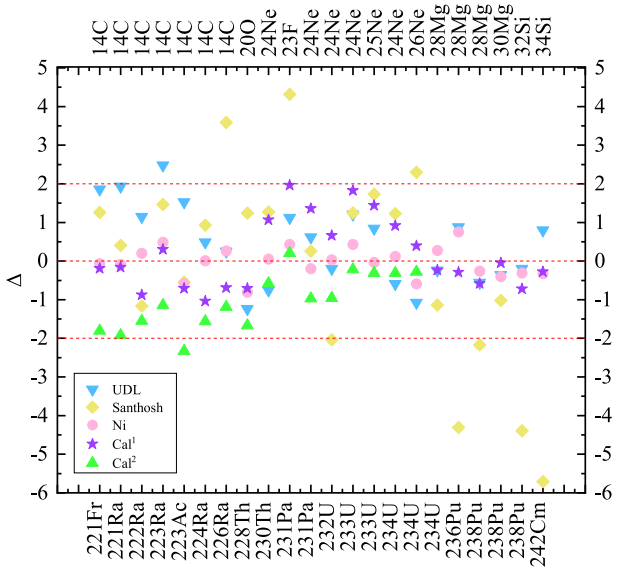

Fig. 1. (color online) Comparison of the discrepancy in logarithmical form between the experimental cluster radioactivity half-lives and calculated ones obtained in the UDL, Santhosh's model, Ni's formula, and our model.

Table 2. Standard deviation σ between the experimental data and the calculated ones using different theoretical models and/or formulas for cluster radioactivity.

Model	UDL	Santhosh	Ni	Cal[1]	Cal[2]
$\sigma(A_c < 28)$	1.244	1.880	0.365	1.035	1.256
$\sigma(A_c \geq 28)$	0.569	3.594	0.425	0.423	–
σ	1.102	2.469	0.382	0.910	–

this model to predict the half-lives for the possible cluster radioactive candidates. The detailed calculated results are given in Table 3. In this table, the indications for the first to seventh columns are similar to Table 1. From Table 3, it is obvious that the predicted results in Cal[1] are closer to those predicted using the UDL and Ni's formula except for the ones predicted using Santhosh's model. Note that most of the predicted results are of the same order of magnitude. For instance, in the case of $^{227}\mathrm{Th}\rightarrow {}^{209}\mathrm{Pb}+{}^{18}\mathrm{O}$, the predicted cluster radioactivity half-lives using the UDL, Santhosh's model, Ni's formula, and Cal[1] are 21.00, 20.59, 21.69, and 21.38, respectively. This implies that our predictions are reliable. This work may provide theoretical direction for future experiment.

In addition, the correlations between the cluster radioactivity half-lives in logarithmical form $\log_{10}T_{1/2}$, penetration probability in logarithmical form $\log(P)$, and daughter neutron number are plotted in Figs. 2 to 5. Figures 2 and 4 represent the cluster radioactivity half-lives in logarithmic form versus the daughter neutron numbers for the ^{14}C emission from Ra isotopes and ^{24}Ne emission from U isotopes, respectively. Figures. 3 and 5

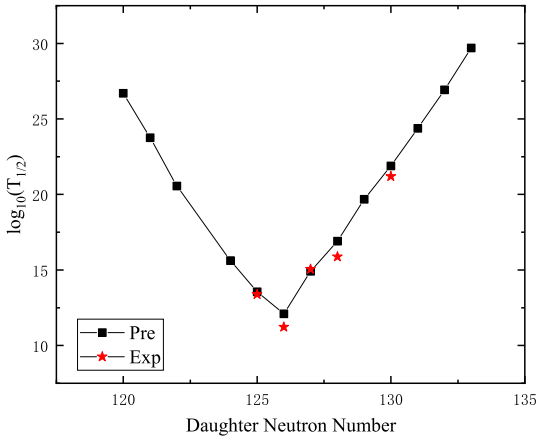

Fig. 2. (color online) Plot of the computed $\log_{10}(T_{1/2})$ values versus neutron numbers of daughter nuclei for the emission of cluster ^{14}C from Ra isotopes. The black squares and red stars represent the predicted and experimental half-lives, respectively.

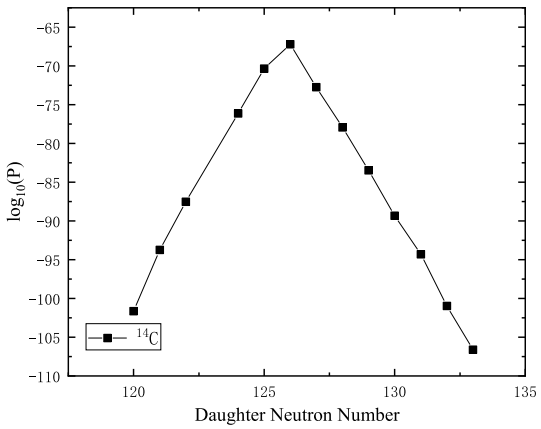

Fig. 3. Plot of the computed $\log_{10}(P)$ values versus neutron numbers of daughter nuclei for the emission of cluster ^{14}C from Ra isotopes.

denote the cluster radioactivity penetration probability in logarithmical form versus the daughter neutron numbers for the ^{14}C emission from Ra isotopes and ^{24}Ne emission from U isotopes, respectively. From Figs. 2 and 4, it is clear that with increasing daughter neutron number, $\log_{10}T_{1/2}$ begins to decrease almost linearly. When it arrives at the magic neutron number 126, the value of $\log_{10}T_{1/2}$ reaches a minimum, then increases linearly again. This is exactly opposite to the tendency for $\log(P)$ depicted in Figs. 3 and 5. Nevertheless, when the daughter neutron number is at the doubly magic daughter nucleus ^{208}Pb, $\log_{10}T_{1/2}$ and $\log(P)$ both take minimum and maximum values. Consequently, this confirms that neutron shell closure plays a more crucial role than proton shell closure in cluster radioactivity, revealing that the neutron pairing effect is more influential than that of protons in this decay mode process [5].

Table 3. Predicted half-lives for possible cluster radioactive nuclei.

Decay	Q_c/MeV	l	$\log_{10}T_{1/2}$ (s)				
			Exp	UDL	Santhosh	Ni	Cal[1]
^{219}Rn→ ^{205}Hg+^{14}C	28.0974	3	−	19.09	15.93	20.29	20.41
^{220}Rn→ ^{206}Hg+^{14}C	28.5380	0	−	17.95	15.44	18.05	18.98
^{221}Fr→ ^{206}Hg+^{15}N	34.1215	3	−	21.55	19.47	22.16	22.06
^{223}Ra→ ^{205}Hg+^{18}O	40.3040	1	−	26.44	22.03	26.41	25.88
^{225}Ra→ ^{211}Pb+^{14}C	29.4661	4	−	17.84	16.13	19.37	19.68
^{225}Ra→ ^{205}Hg+^{20}O	40.4847	1	−	28.27	21.21	28.34	27.59
^{226}Ra→ ^{206}Hg+^{20}O	40.8173	0	−	27.46	20.94	26.41	26.34
^{223}Ac→ ^{208}Pb+^{15}N	39.4720	3	> 14.76	12.93	16.25	14.47	14.53
^{227}Ac→ ^{207}Tl+^{20}O	43.0872	1	−	23.95	19.91	24.55	23.78
^{229}Ac→ ^{206}Hg+^{23}F	48.3458	2	−	28.93	22.43	29.14	27.69
^{226}Th→ ^{208}Pb+^{18}O	45.7293	0	−	18.14	19.35	17.81	18.22
^{226}Th→ ^{212}Po+^{14}C	30.5475	0	> 16.76	17.55	16.55	17.83	18.78
^{227}Th→ ^{209}Pb+^{18}O	44.2021	4	> 15.30	21.00	20.59	21.69	21.38
^{228}Th→ ^{206}Hg+^{22}Ne	55.7416	0	−	27.48	25.37	26.07	25.34
^{229}Th→ ^{209}Pb+^{20}O	43.4038	2	−	24.64	20.60	25.25	24.34
^{229}Th→ ^{205}Hg+^{24}Ne	57.8251	3	−	25.34	23.28	25.72	24.30
^{231}Th→ ^{207}Hg+^{24}Ne	56.2544	2	−	28.12	24.42	28.36	26.54
^{231}Th→ ^{206}Hg+^{25}Ne	56.7977	2	−	27.92	23.69	28.30	26.42
^{232}Th→ ^{208}Hg+^{24}Ne	54.6683	0	> 29.20	31.12	25.57	29.86	28.81
^{232}Th→ ^{206}Hg+^{26}Ne	55.9116	0	> 29.20	30.37	23.99	29.45	28.25
^{227}Pa→ ^{209}Bi+^{18}O	45.8713	2	−	19.16	20.13	20.01	19.48
^{229}Pa→ ^{207}Tl+^{22}Ne	58.9558	2	−	23.31	24.20	23.63	22.31
^{230}U→ ^{208}Pb+^{22}Ne	61.3883	0	> 18.20	20.73	23.62	20.09	19.49
^{230}U→ ^{206}Pb+^{24}Ne	61.3521	0	> 18.20	22.34	22.94	21.78	20.88
^{232}U→ ^{204}Hg+^{28}Mg	74.3195	0	> 22.26	25.59	26.47	24.93	23.45
^{233}U→ ^{205}Hg+^{28}Mg	74.2271	3	> 27.59	25.66	26.57	26.33	24.42
^{235}U→ ^{211}Pb+^{24}Ne	57.3635	1	> 27.65	29.16	25.73	29.51	27.91
^{235}U→ ^{210}Pb+^{25}Ne	57.6832	3	> 27.65	29.41	25.16	29.86	28.25
^{235}U→ ^{207}Hg+^{28}Mg	72.4257	1	> 28.45	28.45	27.65	29.00	26.98
^{235}U→ ^{206}Hg+^{29}Mg	72.4772	3	> 28.45	29.03	27.28	29.67	29.44
^{236}U→ ^{212}Pb+^{24}Ne	55.9451	0	> 26.27	31.83	26.75	30.71	29.38
^{236}U→ ^{210}Pb+^{26}Ne	56.6920	0	> 26.27	32.10	25.54	31.23	29.70
^{236}U→ ^{208}Hg+^{28}Mg	70.7345	0	> 26.27	31.25	28.67	30.33	28.36
^{236}U→ ^{206}Hg+^{30}Mg	72.2719	0	> 26.27	29.94	27.09	29.47	28.74
^{238}U→ ^{208}Hg+^{30}Mg	69.4591	0	−	34.79	28.83	33.98	32.67
^{231}Np→ ^{209}Bi+^{22}Ne	61.9033	3	−	21.37	24.26	21.95	20.47
^{233}Np→ ^{209}Bi+^{24}Ne	62.1600	3	−	22.37	23.48	23.24	21.75
^{235}Np→ ^{207}Tl+^{28}Mg	77.0969	2	−	22.82	26.12	23.92	22.27
^{237}Np→ ^{207}Tl+^{30}Mg	74.7869	2	> 27.57	27.54	26.75	28.63	28.06
^{237}Pu→ ^{209}Pb+^{28}Mg	77.7263	1	−	23.49	26.86	24.66	23.23

Continued on next page

Table 3-continued from previous page

Decay	Q_c (MeV)	l	$\log_{10}T_{1/2}$ (s)				
			Exp	UDL	Santhosh	Ni	Cal[1]
^{237}Pu→ ^{208}Pb+^{29}Mg	77.4527	3	−	24.51	26.67	25.73	25.94
^{237}Pu→ ^{205}Hg+^{32}Si	91.4574	4	−	25.17	29.50	26.48	27.04
^{239}Pu→ ^{209}Pb+^{30}Mg	75.0841	4	−	28.78	27.68	29.89	29.20
^{239}Pu→ ^{205}Hg+^{34}Si	90.8678	1	−	26.83	29.19	28.50	27.90
^{237}Am→ ^{209}Bi+^{28}Mg	79.8484	2	−	22.06	26.76	23.35	21.75
^{239}Am→ ^{207}Tl+^{32}Si	94.5021	3	−	22.65	29.26	24.38	25.11
^{241}Am→ ^{207}Tl+^{34}Si	93.9599	3	> 24.41	24.13	28.92	26.26	25.91
^{240}Cm→ ^{208}Pb+^{32}Si	97.5504	0	−	20.31	29.00	21.09	22.19
^{241}Cm→ ^{209}Pb+^{32}Si	95.3940	4	−	23.19	29.99	25.02	25.65
^{243}Cm→ ^{209}Pb+^{34}Si	94.7881	2	−	24.77	29.69	27.00	26.47
^{244}Cm→ ^{210}Pb+^{34}Si	93.1718	0	−	27.06	30.48	27.89	27.03

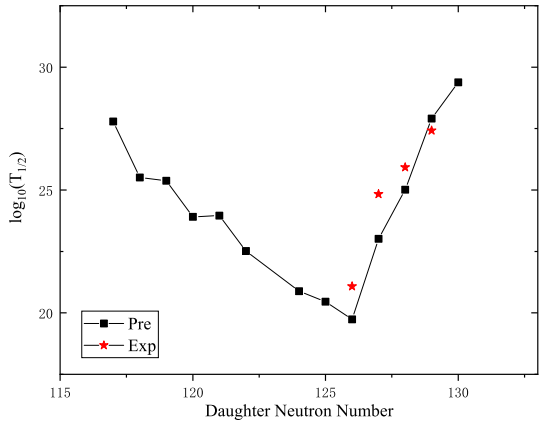

Fig. 4. (color online) Plot of the computed $\log_{10}(T_{1/2})$ values versus neutron numbers of daughter nuclei for the emission of cluster ^{24}Ne from U isotopes. The black squares and red stars represent the predicted and experimental half-lives, respectively.

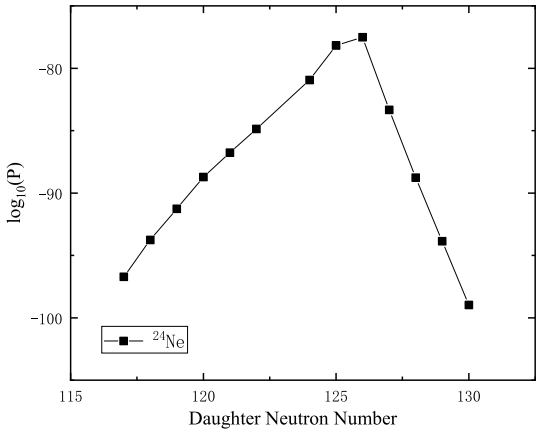

Fig. 5. Plot of the computed $\log_{10}(P)$ values versus neutron numbers of daughter nuclei for the emission of cluster ^{24}Ne from U isotopes.

Furthermore, recent works have shown that the dynamical deformations of the shapes of both the cluster and daughter nuclei are also important in cluster radioactivity [58–63]. The barrier penetration can be changed due to the shape deformations of both the cluster and the residual nuclei in the cluster emission process [58]. The deformations can be reflected in the orientation angle dependent nuclear radius resulting in changes in barrier height [59, 60], which can influence the penetrability and alter the cluster radioactivity half-lives [61–63]. Therefore, it is meaningful to consider dynamical shape deformations of both the cluster and daughter nuclei to study this decay mode. We will also investigate the significance of the dynamical deformations of the shapes of both the cluster and daughter nuclei in cluster radioactivity in more detail in future work.

IV. SUMMARY

In summary, based on the WKB theory, considering the cluster radioactivity preformation probability P_c and using a Woods-Saxon type nuclear potential, we systematically study the half-lives of 22 experimentally observed nuclei. The preformation factor P_c is obtained within CFM applied with the exponential relationship of P_α when $A_c < 28$ and an effective empirical formula when $A_c \geq 28$. The calculated cluster radioactivity half-lives are compared with those obtained by using the UDL, Santhosh's semi-empirical model for both α decay and cluster radioactivity, and Ni's unified formula for both α decay and cluster radioactivity. The results are consistent with the experimental data. Moreover, we extend this model to predict the cluster radioactivity half-lives of the possible candidates. Finally, we confirm the neutron magicity at daughter neutron number 126 and that the neutron pairing effect is more influential than protons in cluster radioactivity.

References

[1] M. Ismail, A. Y. Ellithi, A. E. Depsy *et al.*, Int. J. Mod. Phys. E **26**, 1750026 (2017)
[2] M. Ismail, A. Y. Ellithi, A. E. Depsy *et al.*, Int. J. Mod. Phys. E **25**, 1650069 (2016)
[3] Y. T. Zou, X. Pan, H. M. Liu *et al.*, Phys. Scr. **96**, 075301 (2021)
[4] D. D. Ni and Z. Z. Ren, Phys. Rev. C **82**, 024311 (2010)
[5] M. Ismail, A. Y. Ellithi, M. M. Selim *et al.*, Phys. Scr. **95**, 075303 (2020)
[6] H. F. Zhang, J. M. Dong, G. Royer *et al.*, Phys. Rev. C **80**, 037307 (2009)
[7] Z. Q. Sheng, D. D. Ni, and Z. Z. Ren, J. Phys. G: Nucl. Part. Phys. **38**, 055103 (2011)
[8] K. P. Santhosh, B. Pri, and M. S. Unnikrishnan, Nucl. Phys. A **889**, 29 (2012)
[9] M. Ismail and A. Adel, J. Phys. G: Nucl. Part. Phys. **46**, 075105 (2019)
[10] K. P. Santhosh and T. A. Jose, Pramana-J Phys **95**, 162 (2021)
[11] A. Săndulescu, J. Phys. G: Nucl. Part. Phys. **15**, 529 (1989)
[12] R. K. Gupta and W. Greiner, Int. J. Mod. Phys. E **3**, 335 (1994)
[13] R. Bonetti and A. Guglielmetti, Rom. Rep. Phys. **59**, 301 (2007)
[14] Z. Z. Ren, C. Xu, and Z. J. Wang, Phys. Rev. C **70**, 034304 (2004)
[15] Y. B. Qian and Z. Z. Ren, J. Phys. G: Nucl. Part. Phys. **39**, 015103 (2012)
[16] S. S. Malik and R. K. Gupta, Phys. Rev. C **39**, 1992 (1988)
[17] O. A. P. Tavares and E. L. Medeiros, Phys. Scr. **86**, 015201 (2012)
[18] K. Wei and H. F. Zhang, Phys. Rev. C **102**, 034318 (2020)
[19] D. N. Poenaru and W. Greiner, J. Phys. G: Nucl. Part. Phys. **17**, S443 (1991)
[20] K. P. Santhosh and T. A. Jose, Nucl. Phys. A **992**, 121626 (2019)
[21] K. P. Santhosh and R. K. Biju, Ann. Phys. **334**, 280 (2013)
[22] F. Saidi, M. R. Oudih, M. Fellah *et al.*, Mod. Phys. Lett. A **30**, 1550150 (2015)
[23] G. Royer and R. Moustabchir, Nucl. Phys. A **683**, 182 (2001)
[24] M. Ismail, W. M. Seif, A. Adel *et al.*, Nucl. Phys. A **958**, 202 (2017)
[25] W. M. Seif, M. Shalaby, and M. F. Alrakshy, Phys. Rev. C **84**, 064608 (2011)
[26] W. M. Seif, J. Phys. G: Nucl. Part. Phys. **40**, 105102 (2013)
[27] K. P. Santhosh and T. A. Jose, Phys. Rev. C **99**, 064604 (2019)
[28] M. Balasubramaniam, S. Kumarasamy, N. Arunachalam *et al.*, Phys. Rev. C **70**, 017301 (2004)
[29] A. Singh, A. Shukla, and M. K. Gaidarov, J. Phys. G: Nucl. Part. Phys. **49**, 025101 (2022)
[30] D. D. Ni, Z. Z. Ren, T. K. Dong *et al.*, Phys. Rev. C **78**, 044310 (2008)
[31] R. Kumar, Phys. Rev. C **86**, 044612 (2012)
[32] R. Kumar and M. K. Sharma, Phys. Rev. C **85**, 054612 (2012)
[33] M. Balasubramaniam and N. Arunavhalam, Phys. Rev. C **71**, 014603 (2005)
[34] M. Balasubramaniam and N. S. Rajeswari, Int. J. Mod. Phys. E **23**, 1450018 (2014)
[35] S. M. S. Ahmed, Nucl. Phys. A **962**, 103 (2017)
[36] H. M. Liu, J. Y. Xu, J. G. Deng *et al.*, Int. J. Mod. Phys. E **28**, 1950089 (2019)
[37] S. M. S. Ahmed, R. Yahaya, and S. Radiman, Rom. Rep. Phys. **65**, 1281 (2013)
[38] R. Blendowske and H. Walliser, Phys. Rev. Lett. **61**, 1930 (1988)
[39] K. Wei and H. F. Zhang, Phys. Rev. C **96**, 021601 (2017)
[40] K. P. Santhosh and T. A. Jose, Indian. J. Phys **95**, 121 (2021)
[41] M. Ismail, A. Y. Ellithi, M. M. Selim *et al.*, J. Phys. G: Nucl. Part. Phys. **47**, 055105 (2020)
[42] H. G. de Carvalho, J. B. Martins, and O. A. P. Tavares, Phys. Rev. C **34**, 2261 (1986)
[43] S. Kumar and R. K. Gupta, Phys. Rev. C **55**, 218 (1997)
[44] Y. J. Shi and W. J. Swiatecki, Phys. Rev. Lett. **54**, 300 (1985)
[45] G. Royer, J. Phys. G: Nucl. Part. Phys. **26**, 1149 (2000)
[46] M. Wang, W. J. Huang, F. G. Kondev *et al.*, Chin. Phys. C **45**, 030003 (2021)
[47] F. G. Kondev, M. Wang, W. J. Huang *et al.*, Chin. Phys. C **45**, 030001 (2021)
[48] A. Zdeb, M. Warda, and K. Pomorski, Phys. Rev. C **87**, 024308 (2013)
[49] H. M. Liu, Y. T. Zou, X. Pan *et al.*, Phys. Scr. **96**, 125322 (2021)
[50] D. M. Deng, Z. Z. Ren, D. D. Ni *et al.*, J. Phys. G: Nucl. Part. Phys. **42**, 075106 (2015)
[51] S. M. S. Ahmed, R. Yahaya, S. Radiman *et al.*, J. Phys. G: Nucl. Part. Phys. **40**, 065105 (2013)
[52] J. G. Deng, J. C. Zhao, P. C. Chu *et al.*, Phys. Rev. C **97**, 044322 (2018)
[53] D. M. Deng and Z. Z. Ren, Phys. Rev. C **93**, 044326 (2016)
[54] C. Qi, F. R. Xu, R. J. Liotta *et al.*, Phys. Rev. C **80**, 044326 (2009)
[55] K. P. Santhosh and B. Priyanka, Eur. Phys. J. A **49**, 66 (2013)
[56] K. P. Santhosh, R. K. Biju, and A. Joseph, J. Phys. G: Nucl. Part. Phys. **35**, 085102 (2008)
[57] G. L. Zhang, Y. J. Yao, M. F. Guo *et al.*, Nucl. Phys. A **951**, 86 (2016)
[58] V. Yu. Denisov, Phys. Rev. C **88**, 044608 (2013)
[59] A. Adel and T. Alharbi, Nucl. Phys. A **958**, 187 (2017)
[60] G. Sawhney, M. K. Sharma, and R. K. Gupta, Phys. Rev. C **83**, 064610 (2011)
[61] M. Ismail, W. M. Seif, and A. Abdurrahman, Phys. Rev. C **94**, 024316 (2016)
[62] M. Mirea, A. Săndulescu, and D. S. Delion, Eur. Phys. J. A **48**, 86 (2012)
[63] M. Ismail and A. Adel, J. Phys. G: Nucl. Part. Phys. **49**, 075102 (2022)